ACS Photonics

pubs.acs.org/journal/apchd5

Perspective

Spatiotemporal Optical Vortices: Toward Tailoring Orbital Angular Momentum of Light in Full Space-Time

Wei Chen, Yuan Liu, and Yan-Qing Lu*

Cite This: *ACS Photonics* 2023, 10, 2011−2019

Read Online

ACCESS | Metrics & More | Article Recommendations

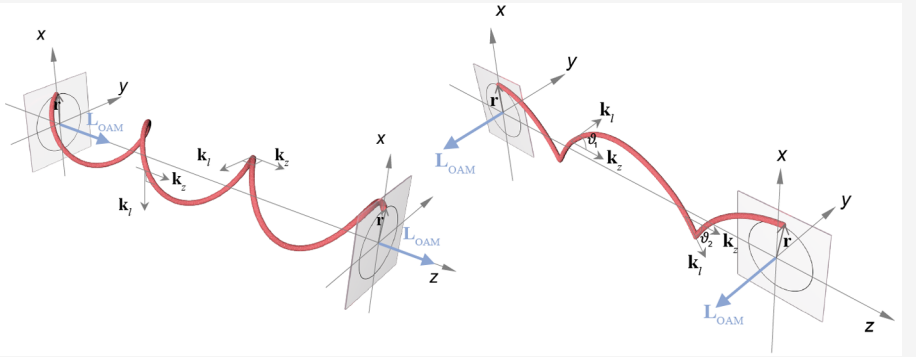

ABSTRACT: Longitudinal orbital angular momentum (OAM) is a fundamental property of light that has been the subject of extensive research and applied to diverse important applications, such as optical tweezers, super-resolution imaging, and optical information processing. Recently, photons have been observed to possess transverse OAM, where the OAM vector is orthogonal to the direction of light propagation. As the carrier for this unique OAM, the spatiotemporal (ST) optical vortex has attracted considerable interest. Here, we provide a general overview of recent experimental and theoretical advances on such vortices, presenting their synthesis and measurement strategies, highlighting their nontrivial properties in linear propagation and interaction with nonlinear matter, and discussing the possible future trends and challenges.

KEYWORDS: *transverse OAM, spatiotemporal OAM, spatiotemporal coupling, time-symmetrical evolution, time diffraction, intrinsic dispersion, time-varying*

INTRODUCTION

Vortices are structures widely seen in nature and science, including quantum vortices in liquid nitrogen, eddies in the water, hurricanes on the ocean, Jupiter's Great Red Spot, and gravitational vortices around black holes. In 1992, Allen et al.[1] proposed that an optical vortex with a phase factor $\exp(il\theta)$ (θ is the azimuth angle) carries orbital angular momentum (OAM) with a value of $l\hbar$ per photon, where $\hbar$ is the Dirac constant and l can be any integer, known as the topological charge. Since the arbitrary value of topological charge provides a new degree of freedom for manipulating light and its interaction with matter, the research on optical vortices attracts considerable attention and continues to deepen, from conventional spiral phase plates to integrated metasurfaces[2] and microring resonators,[3] from particle manipulation[4] to OAM-based communication[5] and quantum information processing,[6] beyond traditional two-dimensional transverse fields to multidimensional tailored beams, especially the time-space modulation of optical vortices.[7−9]

The discovery of optical transverse OAM is a natural consequence of these research extensions.[10−14] Unlike conventional longitudinal OAM, the transverse OAM vector is perpendicular to the direction of light propagation instead of parallel. Since the corresponding light field is essentially a polychromatic optical wave packet, it is also named "spatiotemporal (ST) optical vortex" (for convenience, we refer to it as "ST vortex" in the following text). Such a transverse OAM beam provides great potential to extend the applications of longitudinal OAM and to promote the progress of optics or other basic physics. In this Perspective, we briefly review the historical development of ST vortices and describe in detail different approaches for their efficient generation and characterization. Then we report various new results for ST vortices, including their propagation dynamics, nonlinear interaction

Special Issue: Photonics in China

Received: September 29, 2022
Revised: January 9, 2023
Accepted: January 10, 2023
Published: January 25, 2023

https://doi.org/10.1021/acsphotonics.2c01524
ACS Photonics 2023, 10, 2011−2019

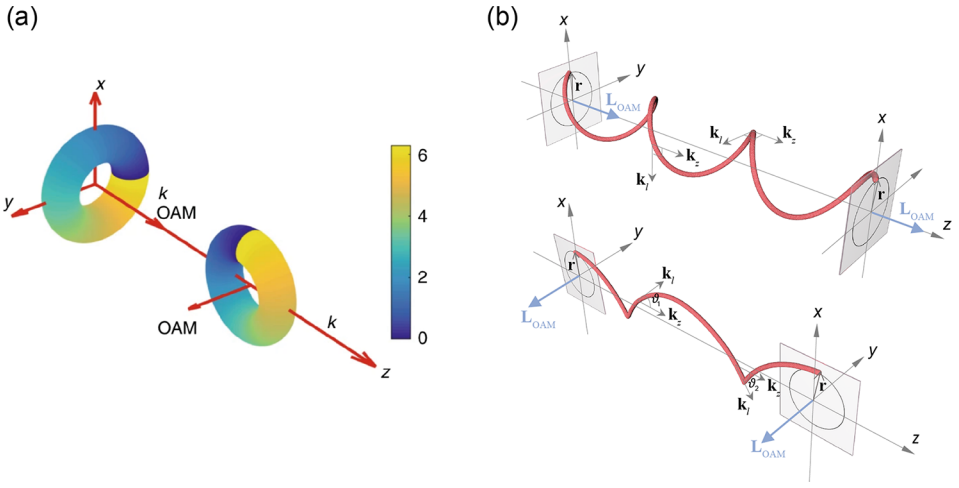

Figure 1. Comparison of longitudinal and transverse OAM. (a) Three-dimensional profiles of the longitudinal OAM beam and the transverse OAM beam. The color bar shows the phase. Adapted with permission from ref 14. Copyright 2020 Nature Publishing Group. (b) (top) For a monochromatic longitudinal OAM beam, the local wavevector $\mathbf{k}_l$ is always perpendicular to the propagation vector $\mathbf{k}_z$. (bottom) For a transverse OAM beam, the monochromaticity is broken due to the interaction of the local wavevector $\mathbf{k}_l$ and the propagation vector $\mathbf{k}_z$. The spiral and cycloid curves represent the linear momentum vectors $\mathbf{p}$ in the above two cases, which donate the OAM by $\mathbf{L}_{OAM} = \mathbf{r} \times \mathbf{p}$. Adapted with permission from ref 15. Copyright 2022 Nature Publishing Group, http://creativecommons.org/licenses/by/4.0/.

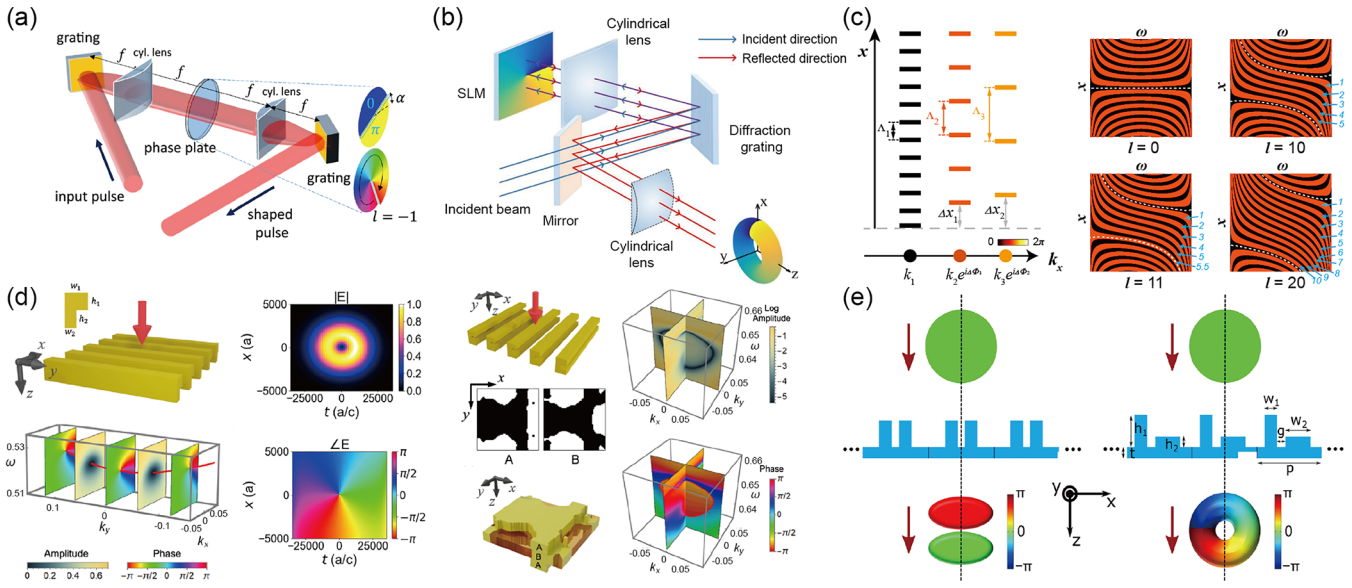

Figure 2. Some methods for ST vortices generation. (a) 4*f*-pulse-shaper-based ST vortices generator consisting of two gratings, two cylindrical lenses, and a phase plate. Adapted with permission from ref 13. Copyright 2021 Optica Publishing Group, https://creativecommons.org/licenses/by/4.0/. (b) Another optical setup that is similar to (a). Adapted with permission from ref 14. Copyright 2020 Nature Publishing Group. (c) (left) Principle of the inverse design of the phase in the immediate x–ω modulation method. (right) Phase patterns for ST vortices generation with controllable topological charges of l = 10, 25, 50, and 100 produced by the x–ω modulation. Adapted with permission from ref 15. Copyright 2022 Nature Publishing Group, https://creativecommons.org/licenses/by/4.0/. (d) (left) A photonic crystal slab design and its transmission spectrum function for generating pulses with transverse OAM. (right) Another design for transverse OAM generator with a photonic crystal slab that is symmetric in both y and z directions. Adapted with permission from ref 19. Copyright 2021 Optica Publishing Group, https://creativecommons.org/licenses/by/4.0/. (e) (left) A one-dimensional periodic structure with a mirror symmetry about the plane $x = 0$ (indicated by the dashed line) cannot generate ST vortices. (right) Breaking mirror symmetry of this one-dimensional structure leads to a singularity in the phase distribution of the transmitted pulse, thereby producing an ST vortex. Reprinted with permission from ref 20. Copyright 2022 Wiley-VCH.

with matter, and rapidly emerging novel ST vortices. We also discuss the possible applications and development prospects of this exciting emerging field, as well as some challenges.

FORM LONGITUDINAL OAM TO TRANSVERSE OAM

From Figure 1a, one immediately sees the intuitive difference between the longitudinal and transverse OAM beams, in which the OAM vector of the latter is rotated by 90° relative to the former, becoming perpendicular to the x–z (or x–τ) plane (instead of the conventional x–y plane). For such a transverse OAM beam, the corresponding optical field can be described as

$$E(x, y, z; \tau) = A(x, y, z; \tau)\exp(il\varphi_{x-\tau}) \quad (1)$$

where $A(x, y, z; \tau)$ is the amplitude of the light field, $\phi_{x-\tau}$ is the azimuth angle in the x–τ plane, $\tau = t - z/v_g$ is the local time

https://doi.org/10.1021/acsphotonics.2c01524
ACS Photonics 2023, 10, 2011−2019

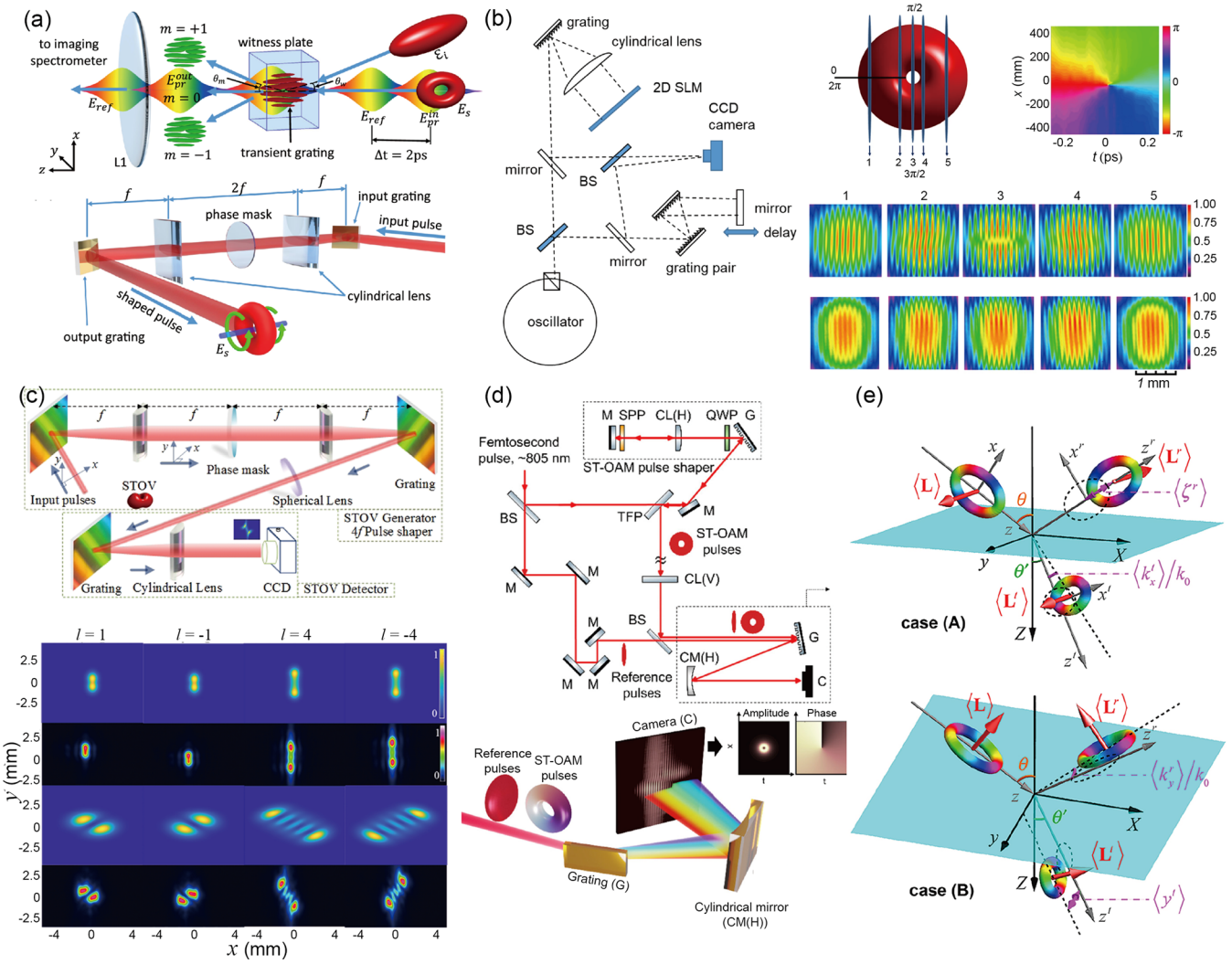

Figure 3. Some measurement methods for ST vortices. (a) Setup for the TG-SSSI, in which a high pulse energy of E_s (>3 μJ) and three extra reference beams (i.e., $\mathcal{E}_i$, E_{ref}, and E_{pr}^{in}) are required. Reprinted with permission from ref 22. Copyright 2021 Optica Publishing Group. (b) (left) Time-resolved filed profile analyzer based on a Mach–Zehnder interferometer consisting of two beam splitters, a CCD camera, and a motorized translation stage in the reference path. (right) Typical results for measuring an ST vortex, in which temporal slices at each time delay are extracted from measured interference patterns and then stacked to reconstruct the full intensity and phase information. Adapted with permission from ref 14. Copyright 2020 Nature Publishing Group. (c) (top) Optical setup to investigate the diffraction properties of an ST vortex. (bottom) Intensity profiles and diffraction patterns of ST vortices ($l = \pm1, \pm4$) in the focal plane of a spherical lens and the observed plane. Adapted with permission from ref 25. Copyright 2022 Optica Publishing Group, https://creativecommons.org/licenses/by/4.0/. (d) (top) Setup for the spatially resolved spectral interferometer (SRSI) to fully characterize ST vortices. (bottom) Corresponding three-dimensional drawing, in which the reference and ST vortex pulses ($l = 1$) are shown next to the camera. Adapted with permission from ref 26. Copyright 2022 American Chemical Society. (e) Schematics of the OAM-dependent transverse and longitudinal pulse shifts of the reflection and refraction of an ST vortex at a planar interface. Adapted with permission from ref 27. Copyright 2022 De Gruyter, https://creativecommons.org/licenses/by/4.0/.

coordinate of the pulse, and v_g is the group velocity. Indeed, compared with the increasingly in-depth research of longitudinal OAM, the research on transverse OAM has been neglected for a long time. Before 2016, there only existed a small number of theoretical works.[10,11] In 2016, Jhajj et al.[12] demonstrated theoretically and experimentally that during the nonlinear interaction of intense optical pulses with air, a small part of the nonlinear harmonic field would convert into ST vortices with opposite topological charges of $l = \pm1$, while the field with OAM value of zero still dominated. In 2019, Hancock et al.[13] and Andy Chong et al.[14] independently realized the generation of ST vortices propagating in free space based on an ST spectral modulation technique, thereby triggering a research boom in such transverse OAM beams.

Apart from the intuitive distinction between the two, the significant difference between longitudinal and transverse OAM and the inherent ST coupling within the latter can be clearly seen from the wave vector analysis.[15] Generally, for an optical field carrying OAM, its OAM density can be expressed as[1] $\mathbf{L}_{OAM} = \mathbf{r} \times \mathbf{p}$, where $\mathbf{r}$ is the position vector, and $\mathbf{p}$ is the linear momentum density related to a local wave vector $\mathbf{k}_l$. For a longitudinal OAM beam, the direction of its OAM vector is parallel to the propagation direction, i.e., $\mathbf{L}_{OAM} \| \mathbf{k}_z$, which means that $\mathbf{k}_l$ is always perpendicular to $\mathbf{k}_z$; therefore, there is no coupling between the two (Figure 1b). While for the transverse OAM beam, the $\mathbf{k}_l$ plane is now rotated by 90° to follow the rotation of the OAM vector, becoming the x–z plane. The break of the orthogonal relationship between $\mathbf{k}_l$ and $\mathbf{k}_z$ leads to their strong

https://doi.org/10.1021/acsphotonics.2c01524
ACS Photonics 2023, 10, 2011–2019

interaction and some nontrivial features of an ST vortex, such as a time-varying OAM and time-symmetrical evolution, as we will discuss below.

GENERATION

In the prior works for generating ST vortices in free space,[13,14] a k_x−ω ST modulation method based on the conventional 4f pulse shaper[16] was proposed. As shown in Figure 2a,b, the incident pulses are first transformed into the ST frequency-frequency (k_x−ω) domain through a diffraction grating and a cylindrical lens. Then the ST spectra of the input pulses are modulated by a spiral phase via a phase device (e.g., a spatial light modulator). In this process, the diffraction grating expands the temporal spectra of the input pulses along the y direction, which can be considered as a one-dimensional temporal Fourier transform. Note that the cylindrical lens in the 4f system is just used to collimate or focus the light fields. Therefore, to complete the k_x−ω modulation, a certain distance of propagation or an additional cylindrical lens behind the 4f system is needed, to provide a one-dimensional spatial Fourier transform (SFT).

Although the ST vortices were successfully generated by applying the k_x−ω modulation, the corresponding topological charge was limited to very low, e.g., l = 1, 2. Actually, strong mode degradation was observed for ST vortices with transverse OAM exceeding l = 1. For example, an ST vortex with l = 2 rapidly converted into a field of two l = 1 vortices with two phase singularities. This phenomenon is mainly due to the dependence of the k_x−ω modulation on the additional SFT via the extra cylindrical lens or transmission, which just works well in the Fourier plane of the cylindrical lens or the far field. More importantly, this modulation method is time-delayed due to the need for transmission accumulation, which may disturb the intrinsic wave vector coupling inside the ST vortex and therefore results in strong mode degradation. To overcome this circumstance, our group demonstrated an immediate x−ω modulation method based on the inverse design of the phase, as shown in Figure 2c.[15] We considered from a frequency point in the k_x−ω domain expressed as

$$\tilde{E}(\Omega, k_n) = |E_n|\delta(k_x - k_n)e^{i\phi_n} \tag{2}$$

where $|E_n|$ is the amplitude and ϕ_n is the phase. Its counterpart on the real x axis can be obtained by taking a Fourier transform along the k_x axis, i.e.,

$$\begin{aligned} E(\Omega_n, x) &= F\cdot T\cdot\{\tilde{E}(\Omega_n, k_n)\} \\ &= \frac{1}{2\pi}\int_{-\infty}^{\infty}|E_n|\delta(k_x - k_n)e^{i\phi_n}e^{ik_x x}\,\mathrm{d}k_x \\ &= \frac{1}{2\pi}|E_n|e^{ik_n(x-\frac{\phi_n}{k_n})} \end{aligned} \tag{3}$$

As shown in eq 3 and Figure 2c, each frequency point corresponds to a one-dimensional location-shifted grating, where the corresponding period and displacement are $\Lambda_n = 2\pi/k_n$ and $\Delta x_n = \phi_n/k_n$, respectively. One can see that the SFT is preprocessed in the phase pattern in the x−ω modulation method, thereby immediately generating the STB vortices with no need for extra transmission. Enabled by x−ω modulation, the transverse OAM value of the generated ST vortices reached 10^2 in the experiment, 2 orders of magnitude higher than previously reported results.

Meanwhile, several ST vortex generators based on integrated optics have been theoretically proposed. Due to the significant progress in the fabrication technique of micronano optical devices and their powerful ability to manipulate electromagnetic waves, integrated optical devices such as metamaterials[2,17] and photonic crystal slabs[18] have been widely used to manipulate longitudinal OAM. By engineering the response function, the photonic crystal slab was suggested to generate ST vortices under the incidence of light pulse with a specific polarization[19] (Figure 2d). Junyi Huang et al.[20] proposed that an ST differentiator can be constructed by breaking the mirror symmetry of a one-dimensional structure (shown in Figure 2e), thereby realizing the transverse OAM generator under irradiating vertically by optical pulses. Their latest study also demonstrated that this ST differentiator is topologically protected, which means it can generate ST vortices even in the presence of random defects.[21]

CHARACTERIZATION

For a longitudinal OAM beam, its structure is mainly shown in its typical doughnut-like field profiles in the x−y plane, which could be directly detected by an imaging device such as the charge-coupled device (CCD). Whereas for the transverse OAM beam, the structural characteristics of the light field are veiled in the x−τ plane. Since direct imaging only reflects the time-averaged intensity information, time-resolved characterizing is necessary. Till now, several schemes for measuring ST vortices have been demonstrated. We first introduce the so-called transient grating single-shot supercontinuum spectral interferometry (TG-SSSI), which can be considered an upgraded version of the SSSI with the addition of phase measurement capabilities.[22] Using the TG-SSSI to extract the intensity and phase information on a structured field E_s requires three additional beams, namely, the reference pulse $\mathcal{E}_i$ and two supercontinuum pulses E_{ref} and E_{pr}^{in} with a specific time delay between the two (Figure 3a). First, E_s, $\mathcal{E}_i$, and E_{pr}^{in} are nonlinearly mixed in a cubic medium (the witness plate) to generate filed $E_{pr}^{out} \propto \chi^{(3)}\,(|E_s|^2 + |\varepsilon_i|^2 + E_s^*\varepsilon_i + E_s\varepsilon_i^*)E_{pr}^{in}$, where $\chi^{(3)}$ donates the three-order nonlinear susceptibility. Then the intensity and phase information on E_s recorded in E_{pr}^{out} could be extracted through the interference patterns of E_{ref} and E_{pr}^{out}, thereby realizing the reconstruction of ST vortices. Although TG-SSSI promises a single-shot measurement of the ST amplitude and phase of an ultrashort pulse, its applicability is limiting due to the needing for high pulse energy (the typical E_s pulse energy was >3 μJ) to excite the third-order nonlinear process. At present, Mach−Zehnder scanning interferometry[23,24] is the most widely used method to measure ST vortices, requiring only one reference pulse (Figure 3b). When an ST vortex and the reference pulse overlap in time, the interference fringes are formed and then recorded by a CCD camera. Since the ST vortex was much longer than the reference pulse precompressed to the transform-limited, its temporal slices can be rebuilt by the interference fringes at a specific time delay τ. Hence, a complete three-dimensional ST vortex could be reconstructed by collecting all its temporal slices, as the reference pulse is scanned in the time domain. Additionally, the corresponding phase could be extracted by the measured interference patterns using standard interferogram analysis techniques.

It is well-known that the topological charge of a conventional vortex can be measured by performing an astigmatic transformation using a cylindrical lens. Shunlin Huang et al.[25] suggested that a similar measurement of ST vortices could be realized by a diffraction grating. This process can be considered a one-dimensional time Fourier transform: using a diffraction

https://doi.org/10.1021/acsphotonics.2c01524
ACS Photonics 2023, 10, 2011−2019

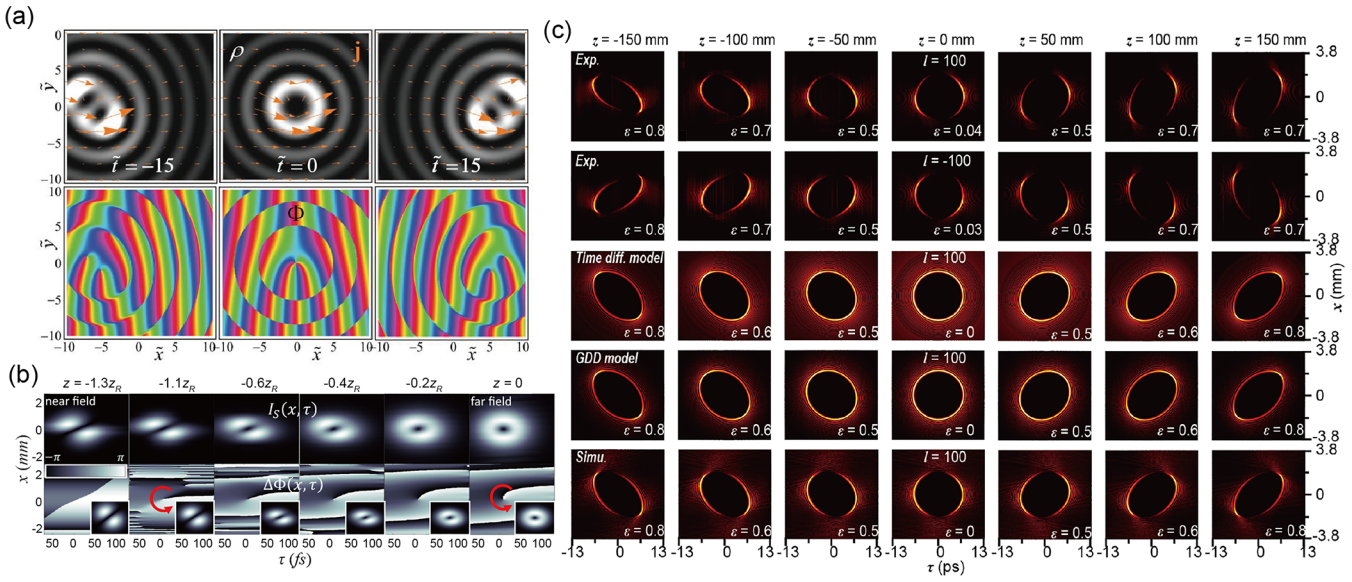

Figure 4. Theoretical and experimental results for propagation dynamics of the ST vortex. (a) (top) Transverse real-space distributions of the intensity ρ and the current **j** for an ST vortex ($l = 2$) at different times. (bottom) Corresponding phases. Adapted with permission from ref 11. Copyright 2012 American Physical Society. (b) Simulated propagation dynamics of an ST vortex with a topological charge of $l = 1$. Adapted with permission from ref 13. Copyright 2019 Optica Publishing Group, https://creativecommons.org/licenses/by/4.0/. (c) Experimental, theoretical, and simulated results of propagation dynamics of two STB vortices with topological charges of $l = \pm 100$. Adapted with permission from ref 15. Copyright 2022 Nature Publishing Group, https://creativecommons.org/licenses/by/4.0/.

grating to expand the temporal spectra of the ST vortex along the y direction. As shown in Figure 3c, the value and sign of the topological charge were reflected as the number of lobes and the stretched direction of the measured diffraction patterns in the x−y plane, respectively. Guan Gui et al.[26] demonstrated that, by introducing an extra reference pulse in the diffraction method, the resulting interference fringes could be used to fully characterize ST vortices with a single frame, while also not requiring strong pulse energy (Figure 3d). Furthermore, OAM-dependent transverse and longitudinal pulse shifts of the reflection and refraction of an ST vortex at a planar interface were investigated recently,[27] which may provide a potential method for characterizing ST vortices (Figure 3e).

PROPAGATION DYNAMICS

Some studies on ST vortices have theoretically predicted their propagation dynamics, indicating that their evolution is similar to the astigmatic transformation of conventional vortex beams but occurs spontaneously in the x−τ plane, with no need for additional devices.[11,13] Interestingly, this behavior has an obvious central position ($\tau = 0$ or $z = 0$), about which the evolution is time-symmetrical (Figure 4a,b). Theoretically, this phenomenon could be explained by the time diffraction model, which describes the different phase accumulation with the transmission of different temporal frequency components within an ST vortex.[11] In this model, an ST Bessel-type (STB) vortex could be considered as the coherent superposition of a series of plane waves,

$$\psi(\vec{r}, t) \propto \int_0^{2\pi} e^{i[k_0 z + \Delta k \cos\tilde{\phi} z + \Delta k \sin\tilde{\phi} x + l\tilde{\phi} - \omega(\tilde{\phi})t]} \, \mathrm{d}\tilde{\phi} \tag{4}$$

where $\omega(\tilde{\phi}) = \mathrm{sqrt}(c^2k_0^2 + c^2\Delta k^2 + 2c^2k_0\Delta k \cos\tilde{\phi})$, c is the speed of light in vacuum, Δk is the spatial bandwidths, and $\psi(\vec{r}, t)$ is the electric field. However, these dynamics lack experimental observation due to the previously mentioned mode degradation induced by the k_x−ω modulation. Fortunately, with the x−ω modulation, our group experimentally observed the predicted time-symmetric evolution of STB vortices, demonstrating pure time diffraction effects on transverse OAM beams (Figure 4c). Inspired by the inherent wavevector interaction within such beams, we further proposed a group dispersion delay (GDD) model to provide a theory-accurately and engineering-friendly description of STB vortices, in which an STB vortex could be expressed as

$$E_l(\rho, \theta; z) = \frac{1}{2\pi}\int_0^{2\pi}\int_0^{\infty} \delta(\kappa - R_0) e^{il\varphi} e^{i/2\beta_2^{\mathrm{int}} z(\kappa\cos\varphi)^2} e^{i\kappa\rho\cos(\varphi-\theta)} \kappa \, \mathrm{d}\kappa \, \mathrm{d}\varphi \tag{5}$$

where the factor $e^{i/2\beta_2^{\mathrm{int}} z(\kappa\cos\varphi)^2}$ donates the GDD. Note that $\beta_2^{\mathrm{int}}(\omega_0)$ is the so-called intrinsic dispersion factor that reads:

$$\beta_2^{\mathrm{int}}(\omega_0) = \left[\gamma^2\left(\frac{\omega_0^2}{c^2} - R_0^2\right) - \frac{R_0^2}{c^2}\right] \Big/ \left(\frac{\omega_0^2}{c^2} - R_0^2\right)^{3/2} \tag{6}$$

where $\gamma = \Delta k_x/\Delta\omega$ and R_0 are the feature parameters of the ST spectra of an ST vortex. The GDD model allows for calculating the intrinsic dispersion factor directly from the ST spectrum, thereby predicting the evolution of an ST vortex. This also helps us to obtain time diffraction-free transverse OAM beams via material dispersion or other effects. Interestingly, in normal dispersive media (such as air), we also found that the transverse OAM of ST vortices does not seem to be conserved but varies with time, whose evolution rate depends on the value of β_2^{int}. This reflects the unique physical characteristics of ST vortices compared with conventional optical vortices.

NONLINEAR INTERACTION

Recently, the research on transverse OAM beams has been extended to the nonlinear domain. A scaling rule similar to the longitudinal OAM was uncovered, in which the Nth harmonic

https://doi.org/10.1021/acsphotonics.2c01524
ACS Photonics 2023, 10, 2011−2019

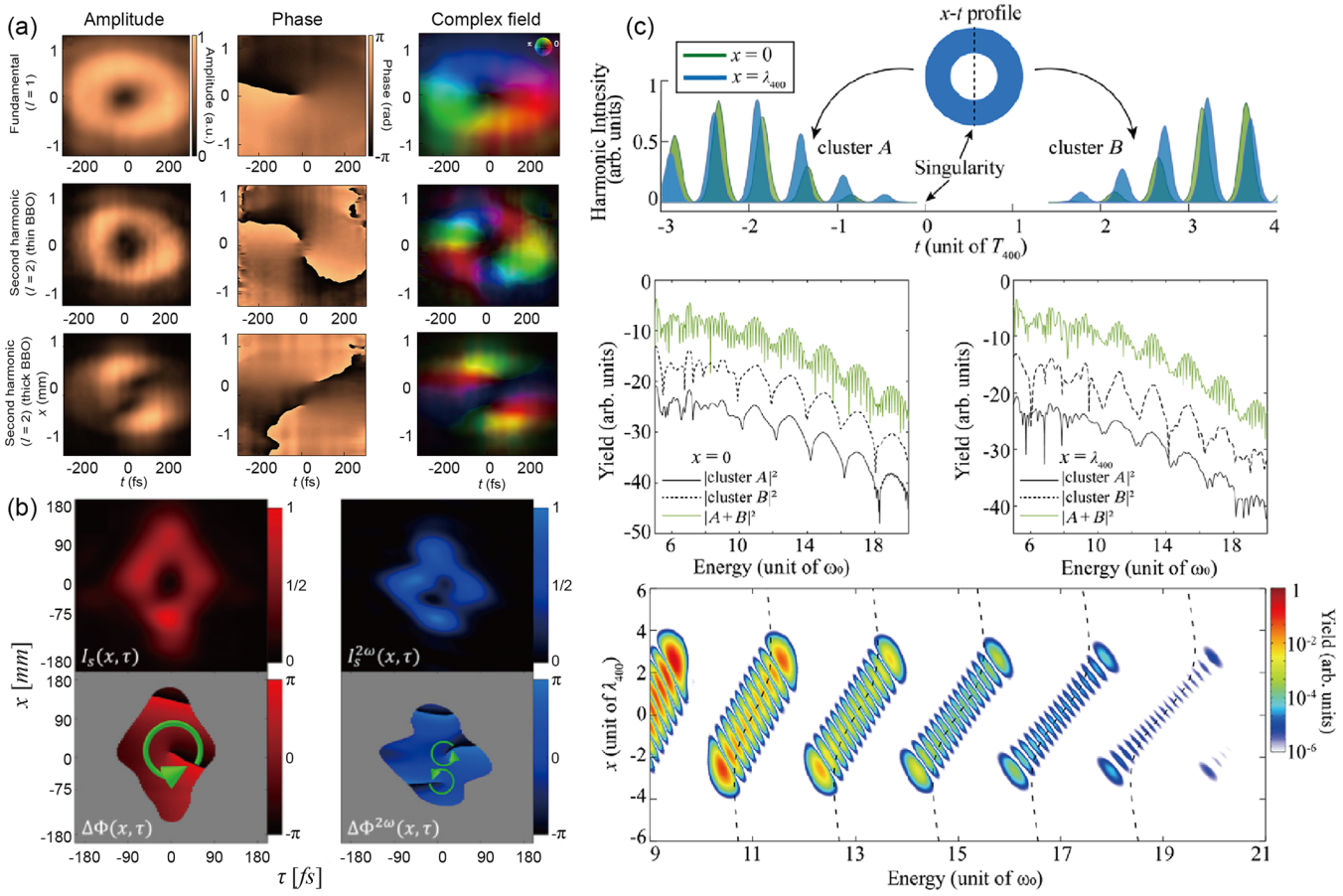

Figure 5. Interaction of ST vortices and nonlinear optical matters. (a) Fundamental ST vortex pulse (l = 1) and its second-harmonic fields generated by (middle) a thin and (bottom) a thick BBO crystal, respectively. Note that the second-harmonic field from the thick BBO crystal exhibits observable mode degradation, indicating the nonconservation of transverse OAM. Reprinted with permission from ref 28. Copyright 2021 Nature Publishing Group. (b) Similar results reported by another group. Reprinted with permission from ref 29. Copyright 2021 Optica Publishing Group, https://creativecommons.org/licenses/by/4.0/. (c) (top) Simulated results for HHG of an ST vortex with a topological charge of l = 1. This indicates the harmonic bursts are separated into cluster A and cluster B in the time domain by the phase singularity of the fundamental ST vortex pulse. (middle) HHG spectra from cluster A, cluster B, and their superposition. (bottom) Spatial-resolved HHG spectrum calculated by the quantum-orbit model. Reprinted with permission from ref 30. Copyright 2021 American Physical Society.

has a topological charge of Nl. As shown in Figure 5a, by cascading a nonlinear barium borate crystal (BBO) at the output of the ST vortex generator, Guan Gui et al.[28] studied the nonlinear second-harmonic generation process of the transverse OAM beams. Hancock et al.[29] demonstrated similar experimental results almost simultaneously (Figure 5b). It can be clearly seen that the ST vortex with l = 1 is converted into the second-harmonic vortex with l = 2 during the nonlinear frequency doubling. This process could be expressed as[28]

$$E^{(2\omega)}(x, y, \tau) = E_0 e^{il^{(2\omega)}\Phi(x,y,\tau)} \propto (E^{(\omega)}(x, y, \tau))^2 \propto (e^{il^{(\omega)}})^2 \propto e^{i2l^{(\omega)}} \tag{7}$$

Remarkably, the second-harmonic vortex generated from a thicker BBO crystal exhibits observable mode degradation and nonconservation of transverse OAM (Figure 5a). The authors claimed that the mode degradation might be due to the mismatch between the spatial diffraction and the material dispersion. Actually, based on the present results, this phenomenon may be explained by a joint effect of the phase mismatch, the time diffraction, and the mode degradation induced by the applied k_x–ω modulation. Another theoretical work from Yiqi Fang et al.[30] turned to the high harmonic generation (HHG) with transverse OAM driven by ST vortices. As shown in Figure 5c, the calculated results indicate that the Nth harmonic carries an ST phase singularity with a topological charge of Nl, thus verifying the above-mentioned scaling rule.

INCREASING THE VARIETY OF ST VORTICES

So far, we mainly discussed the ST vortices having field profiles with one phase singularity under scalar field approximation. In fact, the variety of ST vortices can be significantly enriched by considering more physical variables. Chenhao Wan et al.[31] demonstrated that by setting the phase pattern in the 4f pulse shaper as

$$\phi(x, y) = \tan^{-1}\left(\frac{y}{x + 0.5x_0}\right) - \tan^{-1}\left(\frac{y}{x - 0.5x_0}\right) \tag{8}$$

two ST vortices with different transverse OAMs can be embedded in one wave packet (Figure 6a), thereby realizing a dynamic-transverse-OAM beam (note that in eq 8, x_0 presents the spacing between the two vortices). As shown in Figure 6b, by introducing random phase noise into the ST spectrum, Mirando et al.[32] investigated ST vortices with partial temporal coherence, obtaining a relatively chaotic field profile with phase singularities. Chenhao Wan et al.[33] demonstrated the combina-

https://doi.org/10.1021/acsphotonics.2c01524
ACS Photonics 2023, 10, 2011−2019

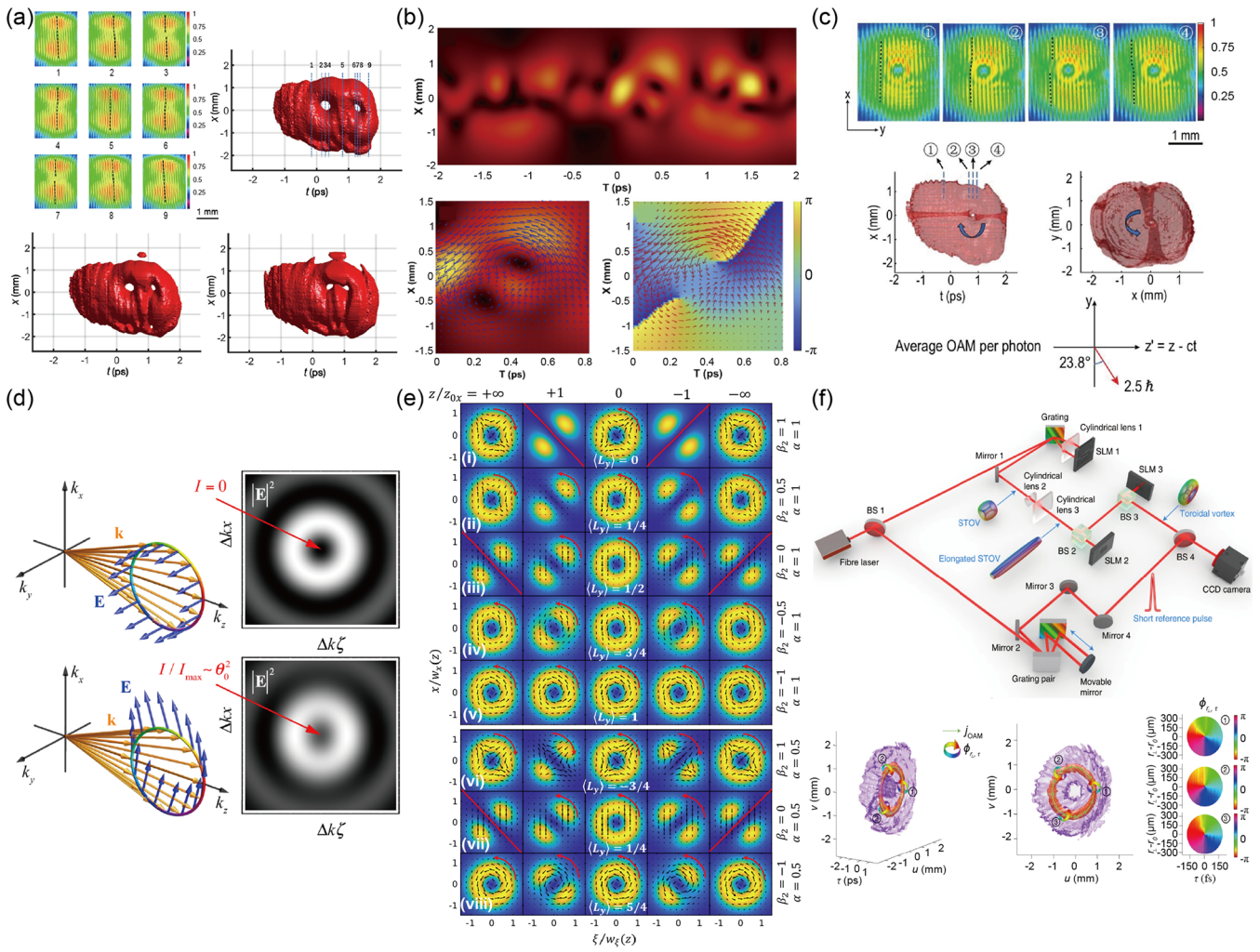

Figure 6. Toward more kinds of ST vortices. (a) ST vortex with dynamic transverse OAM and temporal separation of (top right) 1.00 ps, (bottom left) 0.74 ps, and (bottom right) 0.51 ps. Adapted with permission from ref 31. Copyright 2020 Elsevier B.V. and Science China Press. (b) Partial temporal coherent ST vortex ($l = 2$) with a random spectral phase having a normal distribution. Reprinted with permission from ref 32. Copyright 2021 Optica Publishing Group, https://creativecommons.org/licenses/by/4.0/. (c) Intersection of an ST vortex ($l = 1$) and a conventional spatial vortex ($l = 1$). (top) Interference fringe patterns of the reference pulse with the synthesized field at different times. (bottom) Three-dimensional intensity profiles of the synthesized field from different views. Adapted with permission from ref 33. Copyright 2022 China Science Publishing & Media Ltd., https://creativecommons.org/licenses/by/4.0/. (d) (left) Electric fields of plane waves in the spectra of vector STB vortex for (top) the out-of-plane polarization and (bottom) the in-plane polarization. (right) Corresponding real-space intensity profiles. Reprinted with permission from ref 34. Copyright 2021 American Physical Society. (e) Calculated propagation dynamics for ST vortices with transverse OAM value quantized in integer multiples of $(\alpha-\beta_2/\alpha)/2$, where β_2 is the media dispersion, and α is the eccentricity parameter of the ST vortices. Note the energy density flux $\mathbf{j}$ depicted by black arrows. Reprinted with permission from ref 35. Copyright 2021 American Physical Society. (f) Generation of the photonic toroidal vortex from an ST vortex. (top) Optical setup. (bottom left) Three-dimensional intensity profiles of the toroidal vortex from different views. Note that the ST spiral phase $\Phi_{r_\perp,t}$ is marked with curved colorful arrows, and the local OAM density j_{OAM} is marked with light green arrows. (bottom right) Circulating spiral phase in the radial−temporal plane. Adapted with permission from ref 36. Copyright 2022 Nature Publishing Group, https://creativecommons.org/licenses/by/4.0/.

tion of ST vortices and conventional spatial vortices, in which the resulting field hosts a tilted OAM that provides an additional degree of freedom to the applications that harness the OAM of photons (Figure 6c). The full vector field analysis of STB vortices showed that the distribution of the light field is related to the polarization direction of light.[34] For example, due to the transverse spin−orbit interaction, the in-plane polarization configuration (the filed polarization is parallel to the $x-\tau$ plane) will lead to a nonzero observable intensity in the center of STB vortices (Figure 6d). By analytically solving the OAM value of the ST vortex, S.W. Hancock et al.[35] found that the corresponding transverse OAM is quantized in integer multiples of $\alpha/2$ in vacuum and of $(\alpha-\beta_2/\alpha)/2$ in dispersive media with a dispersion of β_2, where α is the eccentricity parameter that reflects the symmetry of the ST vortex in the $x-\tau$ plane (Figure 6e). This also reflected the nontrivial properties of ST vortices compared with conventional spatial vortices and demonstrated a series of optical fields with a noninteger transverse OAM. Very recently, ST vortices were demonstrated to reshape into toroidal vortices[36] using ray-optics conformal transformation.[37] In this arrangement, STOV pulses are stretched in the direction of their vortex axis, and then their axis is bent within the transverse plane until it closes on itself, forming a ring. As shown in Figure 6f, such a toroidal vortex has a spiral phase that twists around a

https://doi.org/10.1021/acsphotonics.2c01524
ACS Photonics 2023, 10, 2011−2019

closed loop and an azimuthal local OAM density, enriching the physical meaning of the optical OAM.

OUTLOOK

To date, the full potential of the ST vortex is still underexplored. Instead, the journey to discover its novel physical properties and applications is just beginning. A typical example is a debate over whether the transverse OAM value of the circular ST vortex is quantized to a half-integer in vacuum.[34,35,38] Particularly, due to the limited size of the phase mask in the experiment, the generated STB vortices via $x-\omega$ modulation deviate from the theoretical values at low spatial frequencies,[15] which may be optimized by adopting computational holography technology.[39] Although the ST vortex generation based on integrated optics is attractive because it can significantly simplify the whole system, it is still difficult to fabricate due to processing precision, intrinsic material absorption, and other limitations. We note that specially designed metamaterials have recently been used to generate light fields with complex ST structures.[40,41] Therefore, we expect that the compact ST vortex generators are promising and may be an essential research topic in the future.

Many previous studies provided evidence that the ST vortex appears to be an evanescent field in normal dispersive media,[11−15,28,29,34−36] which is not conducive to its practical application. Since the evolution of ST vortices can be quantified as a positive intrinsic dispersion factor,[15] the most direct way to obtain a propagation-invariant ST vortex is to use natural anomalous dispersive materials or construct equivalent optical structures to compensate for the inherent dispersion. Another proven strategy is to generate ST vortices with larger topological charges because the evolution rates will be significantly slower than those with smaller topological charges.[15] Additionally, because the intrinsic dispersion can be reduced by modulating the ST spectrum,[15] the ST vortex that maintains one singularity of zero intensity in a relatively long propagation distance can be obtained with a tailored ST spectrum, but the corresponding integral OAM value may be noninteger.[34] A very speculative solution is to compensate for the intrinsic dispersion using higher-order nonlinear effects, similar to the generation of optical solitons.

The interaction of ST vortices with the matter has more possibilities. For example, wavelength-controllable ST vortex sources and probably entangled states of transverse OAM can be realized using different nonlinear processes. This possibility should be based on fully considering various complex effects in the nonlinear process involving ST vortices, such as phase mismatch, group velocity mismatch, absorption or losses, pump depletion, and so on.[42,43] Spin-determined transverse OAM beams can also be expected by using flexible metamaterials[44,45] or liquid crystal geometric phase devices.[46,47] Additionally, it is possible to enhance and exploit transverse spin−orbit angular momentum coupling by studying ST vortices interacting with chiral matter.[48] The time-varying properties of ST vortices may also be used for coherent control over quantum mechanical methods such as ultrafast chemical reactions[49,50] and for driving or monitoring the motions of molecules via the so-called Raman-active phonons.[51,52] Although it is still too early to predict the roadmap and applications of ST vortices, this burgeoning field is rapidly emerging and is beginning to yield exciting results, which may profoundly change us in understanding and utilizing light in the future.

AUTHOR INFORMATION

Corresponding Author

Yan-Qing Lu − *National Laboratory of Solid State Microstructures, Key Laboratory of Intelligent Optical Sensing and Manipulation, College of Engineering and Applied Sciences, and Collaborative Innovation Center of Advanced Microstructures, Nanjing University, Nanjing 210093, China;* orcid.org/0000-0001-6151-8557; Email: yqlu@nju.edu.cn

Authors

Wei Chen − *National Laboratory of Solid State Microstructures, Key Laboratory of Intelligent Optical Sensing and Manipulation, College of Engineering and Applied Sciences, and Collaborative Innovation Center of Advanced Microstructures, Nanjing University, Nanjing 210093, China*

Yuan Liu − *National Laboratory of Solid State Microstructures, Key Laboratory of Intelligent Optical Sensing and Manipulation, College of Engineering and Applied Sciences, and Collaborative Innovation Center of Advanced Microstructures, Nanjing University, Nanjing 210093, China;* orcid.org/0000-0002-2063-2254

Complete contact information is available at: https://pubs.acs.org/10.1021/acsphotonics.2c01524

Funding

This work has been funded by the National Key Research and Development Program of China (No. 2022YFA1405000), the Natural Science Foundation of Jiangsu Province, Major Project (BK20212004), and the Innovation Program for Quantum Science and Technology (2021ZD0301500).

Notes

The authors declare no competing financial interest.

REFERENCES

(1) Allen, L.; Beijersbergen, M. W.; Spreeuw, R. J. C.; Woerdman, J. P. Orbital angular momentum of light and the transformation of Laguerre-Gaussian laser modes. *Phys. Rev. A* **1992**, *45* (11), 8185−8189.

(2) Sroor, H.; Huang, Y. W.; Sephton, B.; Naidoo, D.; Vallés, A.; Ginis, V.; Qiu, C. W.; Ambrosio, A.; Capasso, F.; Forbes, A. High-purity orbital angular momentum states from a visible metasurface laser. *Nat. Photonics* **2020**, *14* (8), 498−503.

(3) Cai, X.; Wang, J.; Strain, M. J.; Johnson-Morris, B.; Zhu, J.; Sorel, M.; O'Brien, J. L.; Thompson, M. G.; Yu, S. Integrated compact optical vortex beam emitters. *Science* **2012**, *338* (6105), 363−366.

(4) Grier, D. G. A revolution in optical manipulation. *Nature* **2003**, *424* (6950), 810−816.

(5) Lei, T.; Zhang, M.; Li, Y.; Jia, P.; Liu, G. N.; Xu, X.; Li, Z.; Min, C.; Lin, J.; Yu, C.; Niu, H.; Yuan, X. Massive individual orbital angular momentum channels for multiplexing enabled by Dammann gratings. *Light: Sci. Appl.* **2015**, *4* (3), e257.

(6) Mair, A.; Vaziri, A.; Weihs, G.; Zeilinger, A. Entanglement of the orbital angular momentum states of photons. *Nature* **2001**, *412* (6844), 313−316.

(7) Rego, L.; Dorney, K. M.; Brooks, N. J.; Nguyen, Q. L.; Liao, C. T.; San Roman, J.; Couch, D. E.; Liu, A.; Pisanty, E.; Lewenstein, M.; Plaja, L.; Kapteyn, H. C.; Murnane, M. M.; Hernandez-Garcia, C. Generation of extreme-ultraviolet beams with time-varying orbital angular momentum. *Science* **2019**, *364* (6447), eaaw9486.

(8) Sedeh, H. B.; Salary, M. M.; Mosallaei, H. Time-varying optical vortices enabled by time-modulated metasurfaces. *Nanophotonics* **2020**, *9* (9), 2957−2976.

(9) Zhao, Z.; Song, H.; Zhang, R.; Pang, K.; Liu, C.; Song, H.; Almaiman, A.; Manukyan, K.; Zhou, H.; Lynn, B.; Boyd, R. W.; Tur, M.; Willner, A. E. Dynamic spatiotemporal beams that combine two

independent and controllable orbital-angular-momenta using multiple optical-frequency-comb lines. *Nat. Commun.* **2020**, *11* (1), 4099.
(10) Sukhorukov, A.; Yangirova, V. Spatio-temporal vortices: properties, generation and recording. *Proc. SPIE* **2005**, *5949*, 35−43.
(11) Bliokh, K. Y.; Nori, F. Spatiotemporal vortex beams and angular momentum. *Phys. Rev. A* **2012**, *86* (3), 033824.
(12) Jhajj, N.; Larkin, I.; Rosenthal, E. W.; Zahedpour, S.; Wahlstrand, J. K.; Milchberg, H. M. Spatiotemporal optical vortices. *Phys. Rev. X* **2016**, *6* (3), 031037.
(13) Hancock, S. W.; Zahedpour, S.; Goffin, A.; Milchberg, H. M. Free-space propagation of spatiotemporal optical vortices. *Optica* **2019**, *6* (12), 1547−1553.
(14) Chong, A.; Wan, C.; Chen, J.; Zhan, Q. Generation of spatiotemporal optical vortices with controllable transverse orbital angular momentum. *Nat. Photonics* **2020**, *14* (6), 350−354.
(15) Chen, W.; Zhang, W.; Liu, Y.; Meng, F.-C.; Dudley, J. M.; Lu, Y.-Q. Time diffraction-free transverse orbital angular momentum beams. *Nat. Commun.* **2022**, *13* (1), 4021.
(16) Weiner, A. M. Femtosecond pulse shaping using spatial light modulators. *Rev. Sci. Instrum.* **2000**, *71* (5), 1929−1960.
(17) Yu, N.; Genevet, P.; Kats, M. A.; Aieta, F.; Tetienne, J.-P.; Capasso, F.; Gaburro, Z. Light propagation with phase discontinuities: generalized laws of reflection and refraction. *Science* **2011**, *334* (6054), 333−337.
(18) Wang, B.; Liu, W.; Zhao, M.; Wang, J.; Zhang, Y.; Chen, A.; Guan, F.; Liu, X.; Shi, L.; Zi, J. Generating optical vortex beams by momentum-space polarization vortices centred at bound states in the continuum. *Nat. Photonics* **2020**, *14* (10), 623−628.
(19) Wang, H.; Guo, C.; Jin, W.; Song, A. Y.; Fan, S. Engineering arbitrarily oriented spatiotemporal optical vortices using transmission nodal lines. *Optica* **2021**, *8* (7), 966−971.
(20) Huang, J.; Zhang, J.; Zhu, T.; Ruan, Z. Spatiotemporal differentiators generating optical vortices with transverse orbital angular momentum and detecting sharp change of pulse envelope. *Laser Photonics Rev.* **2022**, *16* (5), 2100357.
(21) Huang, J.; Zhang, H.; Zhu, T.; Ruan, Z. Topologically protected generation of spatiotemporal optical vortices with nonlocal spatial-mirror-symmetry-breaking metasurface. *arXiv:2206.01925 [physics.optics]* **2022**, na.
(22) Hancock, S. W.; Zahedpour, S.; Milchberg, H. M. Transient-grating single-shot supercontinuum spectral interferometry (TG-SSSI). *Opt. Lett.* **2021**, *46* (5), 1013−1016.
(23) Li, Y.; Lewellen, J. W. Generating a quasiellipsoidal electron beam by 3D laser-pulse shaping. *Phys. Rev. Lett.* **2008**, *100* (7), 074801.
(24) Li, H.; Bazarov, I. V.; Dunham, B. M.; Wise, F. W. Three-dimensional laser pulse intensity diagnostic for photoinjectors. *Phys. Rev. Spec. Top. -Accel. Beams* **2011**, *14* (11), 112802.
(25) Huang, S.; Wang, P.; Shen, X.; Liu, J.; Li, R. Diffraction properties of light with transverse orbital angular momentum. *Optica* **2022**, *9* (5), 469−472.
(26) Gui, G.; Brooks, N. J.; Wang, B.; Kapteyn, H. C.; Murnane, M. M.; Liao, C.-T. Single-frame characterization of ultrafast pulses with spatiotemporal orbital angular momentum. *ACS Photonics* **2022**, *9* (8), 2802−2808.
(27) Mazanov, M.; Sugic, D.; Alonso, M. A.; Nori, F.; Bliokh, K. Y. Transverse shifts and time delays of spatiotemporal vortex pulses reflected and refracted at a planar interface. *Nanophotonics* **2022**, *11* (4), 737−744.
(28) Gui, G.; Brooks, N. J.; Kapteyn, H. C.; Murnane, M. M.; Liao, C. T. Second-harmonic generation and the conservation of spatiotemporal orbital angular momentum of light. *Nat. Photon* **2021**, *15*, 608−613.
(29) Hancock, S. W.; Zahedpour, S.; Milchberg, H. M. Second-harmonic generation of spatiotemporal optical vortices and conservation of orbital angular momentum. *Optica* **2021**, *8* (5), 594−597.
(30) Fang, Y.; Lu, S.; Liu, Y. Controlling photon transverse orbital angular momentum in high harmonic generation. *Phys. Rev. Lett.* **2021**, *127* (27), 273901.
(31) Wan, C.; Chen, J.; Chong, A.; Zhan, Q. Generation of ultrafast spatiotemporal wave packet embedded with time-varying orbital angular momentum. *Sci. Bull.* **2020**, *65* (16), 1334−1336.
(32) Mirando, A.; Zang, Y.; Zhan, Q.; Chong, A. Generation of spatiotemporal optical vortices with partial temporal coherence. *Opt. Express* **2021**, *29* (19), 30426−30435.
(33) Wan, C.; Chen, J.; Chong, A.; Zhan, Q. Photonic orbital angular momentum with controllable orientation. *Nat. Sci. Rev.* **2022**, *9* (7), No. nwab149.
(34) Bliokh, K. Y. Spatiotemporal Vortex Pulses: Angular momenta and spin-orbit interaction. *Phys. Rev. Lett.* **2021**, *126* (24), 243601.
(35) Hancock, S. W.; Zahedpour, S.; Milchberg, H. M. Mode structure and orbital angular momentum of spatiotemporal optical vortex pulses. *Phys. Rev. Lett.* **2021**, *127* (19), 193901.
(36) Wan, C.; Cao, Q.; Chen, J.; Chong, A.; Zhan, Q. Toroidal vortices of light. *Nat. Photonics* **2022**, *16* (7), 519−522.
(37) Hossack, W. J.; Darling, A. M.; Dahdouh, A. Coordinate transformations with multiple computer-generated optical elements. *J. Mod. Opt* **1987**, *34* (9), 1235−1250.
(38) Bliokh, K. Y. The Enigma of orbital angular momentum of spatiotemporal vortex pulses. *arXiv:2209.04371 [physics.optics]* **2022**, na.
(39) Fienup, J. Iterative method applied to image reconstruction and to computer-generated holograms. *Opt. Eng.* **1980**, *19* (3), 193297.
(40) Shaltout, A. M.; Shalaev, V. M.; Brongersma, M. L. Spatiotemporal light control with active metasurfaces. *Science* **2019**, *364* (6441), eaat3100.
(41) Zdagkas, A.; McDonnell, C.; Deng, J.; Shen, Y.; Li, G.; Ellenbogen, T.; Papasimakis, N.; Zheludev, N. I. Observation of toroidal pulses of light. *Nat. Photonics* **2022**, *16* (7), 523−528.
(42) Boyd, R. W.*Nonlinear Optics*; Academic Press: New York, 1992.
(43) Agrawal, G. P.*Nonlinear Fiber Optics*, 3rd ed.; Academic: New York, U.S.A., 2001.
(44) Ni, J.; Huang, C.; Zhou, L. M.; Gu, M.; Song, Q. H.; Kivshar, Y.; Qiu, C. W. Multidimensional phase singularities in nanophotonics. *Science* **2021**, *374* (6566), No. eabj0039.
(45) Ouyang, X.; Xu, Y.; Xian, M.; Feng, Z.; Zhu, L.; Cao, Y.; Lan, S.; Guan, B.; Qiu, C. W.; Gu, M.; Li, X. Synthetic helical dichroism for six-dimensional optical orbital angular momentum multiplexing. *Nat. Photon* **2021**, *15* (12), 901−907.
(46) Chen, P.; Wei, B. Y.; Hu, W.; Lu, Y. Q. Liquid-crystal-mediated geometric phase: from transmissive to broadband reflective planar optics. *Adv. Mater.* **2019**, *32* (27), 1903665.
(47) Li, Z. X.; Ruan, Y. P.; Chen, P.; Tang, J.; Hu, W.; Xia, K. Y.; Lu, Y. Q. Liquid crystal devices for vector vortex beams manipulation and quantum information applications. *Chin. Opt. Lett.* **2021**, *19* (11), 112601.
(48) Wang, Z.; Cheng, F.; Winsor, T.; Liu, Y. Optical chiral metamaterials: a review of the fundamentals, fabrication methods and applications. *Nanotechnology* **2016**, *27* (41), 412001.
(49) Paul, K.; Sengupta, P.; Ark, E. D.; Tu, H.; Zhao, Y.; Boppart, S. A. Coherent control of an opsin in living brain tissue. *Nat. Phys.* **2017**, *13* (11), 1111−1116.
(50) Gaulier, G.; Dietschi, Q.; Bhattacharyya, S.; Schmidt, C.; Montagnese, M.; Chauvet, A.; Hermelin, S.; Chiodini, F.; Bonacina, L.; Herrera, P. L.; Rothlisberger, U.; Rodriguez, I.; Wolf, J.-P. Ultrafast pulse shaping modulates perceived visual brightness in living animals. *Sci. Adv.* **2021**, *7* (18), No. eabe1911.
(51) Weiner, A. M.; Leaird, D. E.; Wiederrecht, G. P.; Nelson, K. A. Femtosecond pulse sequences used for optical manipulation of molecular motion. *Science* **1990**, *247* (4948), 1317−1319.
(52) Dudovich, N.; Oron, D.; Silberberg, Y. Single-pulse coherently controlled nonlinear Raman spectroscopy and microscopy. *Nature* **2002**, *418* (6897), 512−514.

https://doi.org/10.1021/acsphotonics.2c01524
ACS Photonics 2023, 10, 2011−2019